Earth and Planetary Science Letters 451 (2016) 185–195

Contents lists available at ScienceDirect

Earth and Planetary Science Letters

www.elsevier.com/locate/epsl

Synchronous formation of the metamorphic sole and igneous crust of the Semail ophiolite: New constraints on the tectonic evolution during ophiolite formation from high-precision U–Pb zircon geochronology

Matthew Rioux [a,*], Joshua Garber [a,b], Ann Bauer [c], Samuel Bowring [c], Michael Searle [d], Peter Kelemen [e], Bradley Hacker [a,b]

[a] Earth Research Institute, University of California, Santa Barbara, CA 93106, USA
[b] Department of Earth Science, University of California, Santa Barbara, CA 93106, USA
[c] Department of Earth, Atmospheric and Planetary Science, Massachusetts Institute of Technology, Cambridge, MA 02139, USA
[d] Department of Earth Sciences, University of Oxford, Oxford, OX1 3AN, UK
[e] Department of Earth and Environmental Studies, Columbia University, Lamont Doherty Earth Observatory, Palisades, NY 10964, USA

ARTICLE INFO

Article history:
Received 11 April 2016
Received in revised form 2 June 2016
Accepted 25 June 2016
Available online xxxx
Editor: M. Bickle

Keywords:
ophiolite
Oman
United Arab Emirates
Semail
metamorphic sole
zircon

ABSTRACT

The Semail (Oman–United Arab Emirates) and other Tethyan-type ophiolites are underlain by a sole consisting of greenschist- to granulite-facies metamorphic rocks. As preserved remnants of the underthrust plate, sole exposures can be used to better understand the formation and obduction of ophiolites. Early models envisioned that the metamorphic sole of the Semail ophiolite formed as a result of thrusting of the hot ophiolite lithosphere over adjacent oceanic crust during initial emplacement; however, calculated pressures from granulite-facies mineral assemblages in the sole suggest the metamorphic rocks formed at >35 km depth, and are too high to be explained by the currently preserved thickness of ophiolite crust and mantle (up to 15–20 km). We have used high-precision U–Pb zircon dating to study the formation and evolution of the metamorphic sole at two well-studied localities. Our previous research and new results show that the ophiolite crust formed from 96.12–95.50 Ma. Our new dates from the Sumeini and Wadi Tayin sole localities indicate peak metamorphism at 96.16 and 94.82 Ma (±0.022 to 0.035 Ma), respectively. The dates from the Sumeini sole locality show for the first time that the metamorphic rocks formed either prior to or during formation of the ophiolite crust, and were later juxtaposed with the base of the ophiolite. These data, combined with existing geochemical constraints, are best explained by formation of the ophiolite in a supra-subduction zone setting, with metamorphism of the sole rocks occurring in a subducted slab. The 1.3 Ma difference between the Wadi Tayin and Sumeini dates indicates that, in contrast to current models, the highest-grade rocks at different sole localities underwent metamorphism, and may have returned up the subduction channel, at different times.

1. Introduction

The Semail ophiolite—exposed over approximately 20,000 km^2 in Oman and the United Arab Emirates (UAE)—is the largest and best-studied ophiolite in the world (Fig. 1). The ophiolite preserves a large section of oceanic crust and upper mantle, and has been used extensively to study mid-ocean ridge processes. Current models for the structure of fast-spread oceanic crust and the processes of lower crustal accretion at fast-spreading ridges are based heavily on observations from the ophiolite (e.g., Boudier et al., 1996; Kelemen et al., 1997; Nicolas et al., 1988; Quick and Denlinger, 1993).

Despite the importance of the Semail ophiolite, aspects of its tectonic history remain poorly understood. The large-scale tectonic setting during ophiolite formation is debated, with end-member models envisioning ophiolite formation at a normal mid-ocean ridge spreading center (Boudier et al., 1988) or in a supra-subduction zone setting (Pearce et al., 1981; Searle and Malpas, 1980, 1982). The emplacement history is similarly controversial. The ophiolite is underlain by a sole of amphibolite- to granulite-facies metamorphic rocks that have traditionally been attributed to over-thrusting of the hot ophiolite lithosphere during initial emplacement (Boudier et al., 1988; Hacker et al., 1996); how-

* Corresponding author.
E-mail address: rioux@eri.ucsb.edu (M. Rioux).

http://dx.doi.org/10.1016/j.epsl.2016.06.051
0012-821X/

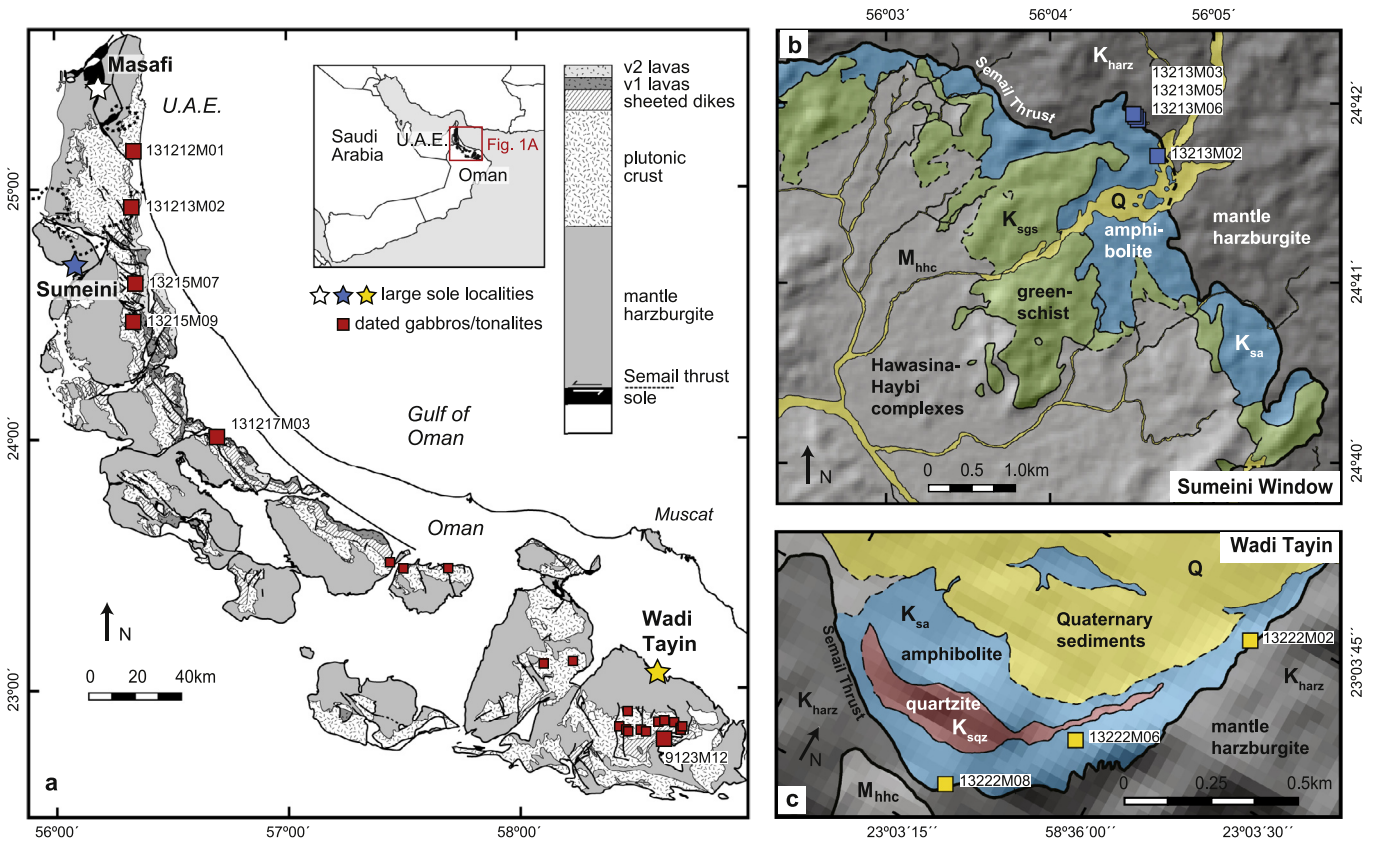

Fig. 1. Geologic maps and sample locations. (a) Geologic map of the Semail (Oman–United Arab Emirates) ophiolite. Insets show location of Fig. 1a and a simplified pseudostratigraphy for the ophiolite. Larger red squares with sample numbers show the locations of plutonic rocks dated in this study and smaller red squares are sample locations of dated ridge-related (V1) plutonic rocks from Rioux et al. (2012, 2013). Map after Nicolas et al. (2000). (b) Lithologic map of the Sumeini Window sole locality. Samples analyzed in this study are identified by blue squares. (c) Lithologic map of the Wadi Tayin sole locality. Samples are identified by yellow squares. For Figs. 1b and 1c, unit boundaries were drawn from multispectral Advanced Spaceborne Thermal Emission and Reflection Radiometer (ASTER) data and Google Earth images, with units assigned based on our field observations and maps from previous studies (Cowan et al., 2014; Searle and Cox, 2002; Searle and Malpas, 1982). Each map is draped over a hillshade derived from the ASTER Global Digital Elevation Model (GDEM) version 2. (A color version of this figure is available with the web version of the article.)

ever, peak metamorphic pressures of 11–13 kbar estimated for granulite mineral assemblages in the sole (Cowan et al., 2014; Gnos, 1998), suggest metamorphism at depths of >35 km—more than can be explained by the currently preserved thickness of ophiolite crust and mantle (up to 15–20 km) (Searle and Cox, 2002). The elevated pressures have been explained by either structural thinning of the ophiolite during or following emplacement (Hacker and Gnos, 1997) or by the formation of the sole rocks within a subducted slab, followed by exhumation up the subduction channel (Searle and Cox, 2002; Searle et al., 2015).

In this study, we used high-precision U–Pb zircon dating and whole rock Sm–Nd isotopic data to better constrain the origin of the metamorphic sole in the Semail ophiolite. We present new dates and isotopic data from the ophiolite crust and two well-studied sole localities. Our data show that sole metamorphism was diachronous, with the earliest metamorphism occurring at the same time or prior to formation of the ophiolite crust. We use the data to constrain the tectonic setting of ophiolite formation and develop new models for the formation of the metamorphic soles in ophiolites.

2. Geology of the Semail ophiolite

The Semail ophiolite preserves a cross section through oceanic lithosphere, including residual mantle harzburgite and dunite; lower and mid-crustal gabbroic rocks; upper crustal sheeted dikes; and submarine pillow basalts and lavas (Fig. 1a) (Nicolas et al., 2000; Pallister and Hopson, 1981). The volcanic rocks within the ophiolite can be divided into two distinct series based on their geochemistry and structural position. V1 (Geotimes unit) pillow basalts and lavas directly overlie the sheeted dike complex. They have geochemical signatures that are most similar to modern mid-ocean ridge basalts (MORB) (Ernewein et al., 1988; Godard et al., 2006), although on average they have lower TiO_2 at a given MgO (MacLeod et al., 2013), and are deleted in Nb and Ta—relative to Th and La—compared to average MORB (e.g., Godard et al., 2006). The V1 volcanic series are interpreted to represent the volcanic equivalent of the main plutonic crust (Haase et al., 2016; Kelemen et al., 1997). The overlying, younger V2 volcanic series (Lasail and Alley units) are depleted in immobile incompatible trace elements (e.g., Nb, Ta, REE, Zr) relative to the V1 series, and have chemical similarities to some highly depleted volcanic rocks formed above subduction zones (Alabaster et al., 1982; Ishikawa et al., 2002; Pearce et al., 1981). Intrusive equivalents of the V2 plutonic series become volumetrically more significant from south to north; the V2 series is present, but makes up a small portion of the crust in the southernmost massifs, whereas up to 50% of the crust in the UAE section of the ophiolite is composed of the V2 magmatic series (Goodenough et al., 2010; Haase et al., 2016; Rioux et al., 2013; Styles et al., 2006). The differences in geochemistry between the V1 and V2 lavas and modern MORB have been one of the primary arguments in favor of a supra-subduction zone origin for the ophiolite (e.g., MacLeod et al., 2013; Pearce et al., 1981).

The metamorphic sole of the Semail ophiolite is exposed in several localities along the eastern and western margins of the

ophiolite (Nicolas et al., 2000; Searle and Malpas, 1980, 1982), with the largest and best-studied sections at the Wadi Tayin, Sumeini and Masafi localities (Fig. 1). At each exposure, the sole is separated from the overlying mantle harzburgite by the Semail thrust. Below the thrust, sole metamorphic rocks record a condensed, inverted metamorphic gradient, reflecting tectonic juxtaposition of rocks metamorphosed at different pressures and temperatures (Gnos, 1998). The highest-grade rocks consist of amphibolites with rare granulite enclaves in a m-scale band directly below the Semail thrust. Cm-scale diorite to tonalite pods and dikes occur at the highest structural levels and have been interpreted as small-volume intrusions formed by melting during peak metamorphism (Cowan et al., 2014; Searle and Malpas, 1980). Petrological and geochemical analyses indicate that the amphibolites are metamorphosed MORB that are chemically different than the over-thrust ophiolite crust (Searle and Malpas, 1982). The amphibolites are underlain by a thicker sequence of dominantly meta-sedimentary lower amphibolite to greenschist-facies marbles and quartzites. Pressure–temperature estimates from the sole range from 770–900 °C and 11–13 kbar for granulite-facies mineral assemblages within the amphibolites; 700–750 °C and 9 kbar for upper amphibolite-facies mineral assemblages; and 475–550 °C and 4.5–5.5 kbar for the lower amphibolite- to greenschist-facies metasediments (Cowan et al., 2014; Gnos, 1998; Hacker and Mosenfelder, 1996). The sole rocks are underlain by lower grade sedimentary and volcanic rocks of the Haybi and Hawasina complex thrust sheets (Fig. 1).

3. Existing geochronology

Our work builds on previous geochronologic studies of the ophiolite crust and metamorphic sole. In the $^{40}Ar/^{39}Ar$ system, Hacker et al. (1996) presented a large dataset of amphibole and mica cooling dates from the ophiolite. The data showed that sole metamorphism was synchronous with or rapidly followed formation of the ophiolite crust, but were not precise enough to differentiate between these alternatives; the authors interpreted the data to reflect formation of the metamorphic sole as a result of rapid thrusting of the ophiolite over adjacent oceanic crust.

Three previous studies have used multigrain isotope-dilution-thermal-ionization mass spectrometry (ID-TIMS) U–Pb zircon dating to study the ophiolite. Tilton et al. (1981) carried out the first dating of plutonic rocks in the ophiolite crust, and reported $^{206}Pb/^{238}U$ dates of 97.3 ± 0.4 to 93.5 ± 0.4 Ma, with most dates clustered around 95 Ma. Warren et al. (2005) re-dated samples from four of the Tilton et al. (1981) localities and found similar $^{206}Pb/^{238}U$ dates of 95.50 ± 0.24 to 94.37 ± 0.18 Ma; some samples from the Tilton et al. (1981) and Warren et al. (2005) studies may be from late V2 plutonic rocks that postdate the main (V1) phase of crust-forming magmatism (Rioux et al., 2013). Warren et al. (2005) further reported a date of 94.48 ± 0.23 Ma for the timing of metamorphism at the Wadi Tayin sole locality, based on combined U–Pb zircon dates from an amphibolite and a small volume trondhjemite pod. Styles et al. (2006) reported zircon U–Pb dates from the UAE portion of the ophiolite: $^{206}Pb/^{238}U$ dates from the late V2 magmatic series ranged from 96.40 ± 0.29 to 94.74 ± 0.54 Ma, and two dates from the Masafi sole locality range from 95.29 ± 0.21 to 95.69 ± 0.25 Ma. Each of the U–Pb datasets suggests that sole metamorphism post-dated the main phase (V1) of ridge magmatism; however, more-detailed conclusions are limited by the precision of the dates and by uncertainties in the intercalibration among the different studies. Dates summarized above are $^{206}Pb/^{238}U$ dates or Isoplot 'concordia dates', as reported in the original publications and are not Th-corrected.

The data presented herein are the most recent results from our group's efforts to generate a large internally consistent dataset of high-precision single-grain U–Pb zircon dates, to constrain the detailed magmatic and tectonic development of the ophiolite. In our previous work, we dated 18 plutonic samples from the main phase of crust-forming magmatism (V1) in the southern ophiolite massifs and seven additional plutonic samples that we attributed to late (V2) magmatism based on field relations (Rioux et al., 2012, 2013). There is a resolvable range of zircon dates in many samples, potentially reflecting either protracted zircon crystallization, or inheritance of zircons from older portions of the magmatic system or surrounding wallrocks (Rioux et al., 2012, 2013). We take the youngest cluster of dates in each sample to be the best estimate of the final crystallization age; all of the dated zircons were analyzed using the chemical abrasion method (Mattinson, 2005), which minimizes the potential for inaccurate younger dates due to Pb-loss. For the V1 magmatism, weighted mean $^{206}Pb/^{238}U$ dates of the youngest dates in each sample range from 96.121 ± 0.051 to 95.504 ± 0.031 Ma. For the V2 magmatism, weighted mean $^{206}Pb/^{238}U$ dates from six samples range from 95.447 ± 0.092 to 95.240 ± 0.025 Ma; one additional sample yielded a range of dates with a minimum zircon $^{206}Pb/^{238}U$ date of 95.067 ± 0.062 Ma. A single trondhjemite dike that intrudes the mantle section just below the crust–mantle boundary in the ophiolite, and has a distinctly lower $\varepsilon_{Nd}(t) = -7.7$, yielded a weighted mean $^{206}Pb/^{238}U$ date of 95.174 ± 0.039 Ma. Finally, we also re-dated the trondhjemite pod from the Wadi Tayin sole locality previously dated by Warren et al. (2005), and found a $^{206}Pb/^{238}U$ date of 94.69 ±

Table 1
Sample locations and descriptions.

Sample	UTM (E)[a]	UTM (N)[a]	IGSN[b]	Location[c]	Rock type
Metamorphic sole					
13213M02	406652	2731521	MER302132	Sumeini, Oman	Discordant diorite vein
13213M03	406443	2731917	MER302133	Sumeini, Oman	Garnet amphibolite
13213M05	406406	2731944	MER302135	Sumeini, Oman	Concordant diorite pod
13213M06	406445	2731904	MER302136	Sumeini, Oman	Concordant diorite pod
13222M02	664130	2551297	MER302222	Wadi Tayin, Oman	Concordant diorite pod
13222M06	663854	2550840	MER302226	Wadi Tayin, Oman	Garnet muscovite schist
13222M08	663609	2550565	MER302228	Wadi Tayin, Oman	Garnet amphibolite
Ophiolite crust					
9123M12	666035	2522009	MER912312	Wadi Tayin massif, Oman	Tonalite
13215M07	433147	2722934	MER302157	Fizh massif, Oman	Gabbro
13215M09	432265	2706321	MER302159	Fizh massif, Oman	Gabbro
131217M03	468789	2655279	MER312173	Sarami massif, Oman	Gabbro
131212M01	432654	2781224	MER312121	Khawr Fakkan massif, UAE	Mirbah gabbro
131213M02	431676	2756913	MER312132	Aswad massif, UAE	Kalba gabbro

[a] WGS 84, UTM zone 40.
[b] Assigned international geo sample number (IGSN).
[c] UAE, United Arab Emirates.

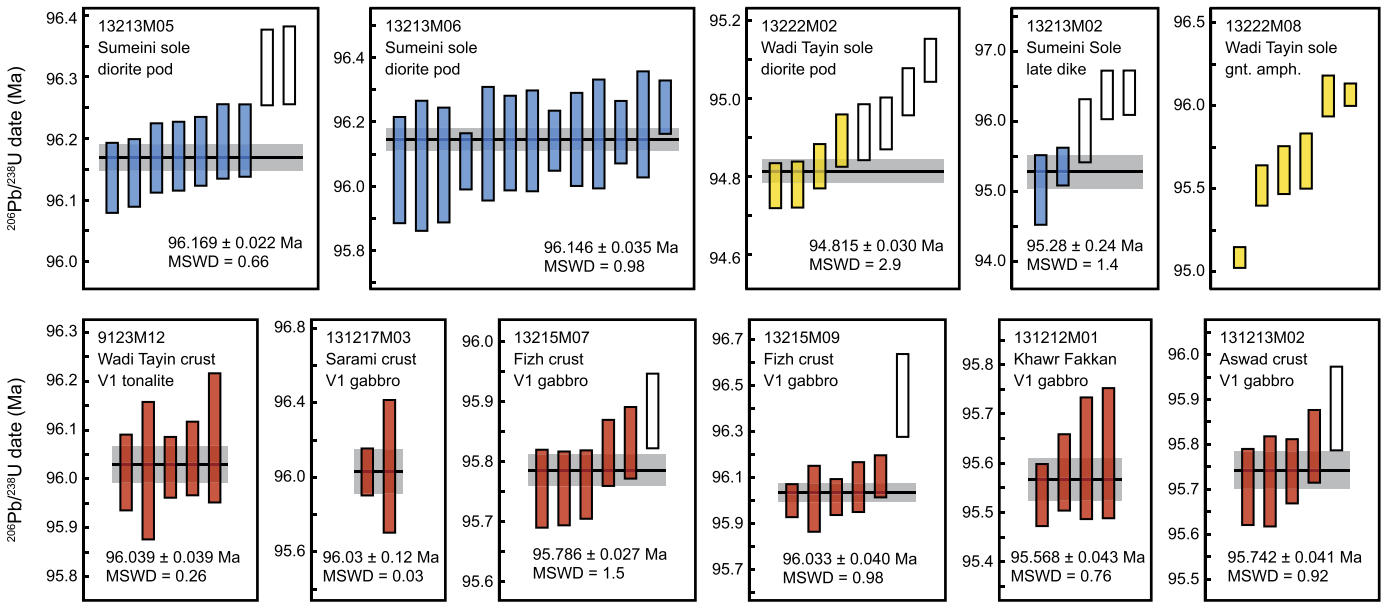

Fig. 2. New Th-corrected ^{206}Pb/^{238}U dates from the V1 plutonic crust and metamorphic sole. Each bar corresponds to a single zircon date $\pm 2\sigma$ uncertainties. Reported dates are weighted mean ^{206}Pb/^{238}U dates $\pm 2\sigma$ uncertainties, calculated from multiple single zircon analyses; open plot symbols were excluded from the weighted mean calculations. Imprecise single zircon analyses were excluded from the plots for clarity (Supplementary Text; Supplementary Table 1). Dates are in millions of years (Ma). MSWD, mean square of the weighted deviates; gnt. amph., garnet amphibolite. (A color version of this figure is available with the web version of the article.)

0.11 Ma. Here we present the first high-precision dates from the Sumeini sole locality, more-precise dates from the Wadi Tayin locality and new dates from the main phase of crustal magmatism in the northern portion of the ophiolite; together, these dates provide important new insights into the formation of the metamorphic sole and the tectonic setting during ophiolite growth.

4. Methods

Single-zircon U–Pb dating was carried out by ID-TIMS in the Radiogenic Isotope Laboratory at the Massachusetts Institute of Technology (MIT). All zircons were dissolved using the chemical abrasion method (Mattinson, 2005), modified for single grain analyses. Analytical methods are described in the Supplementary Text and Rioux et al. (2012). ^{206}Pb/^{238}U dates reported and plotted throughout from this study and Rioux et al. (2012, 2013) are Th-corrected (Supplementary Text). Data from our previous studies discussed herein were recalculated to be consistent with the reduction parameters used in this study. Whole rock Sm–Nd isotopic data were collected at MIT following the procedures outlined in Rioux et al. (2012). Cathodoluminescence (CL) and backscattered electron (BSE) images were collected on the FEI Quanta 400F field-emission scanning electron microscope (SEM) at the University of California, Santa Barbara (UCSB; CL and BSE) and the JEOL Superprobe JXA-733 at MIT (CL).

5. Results

5.1. U–Pb zircon geochronology

Our previous research on the timing of crustal growth focused on the southern ophiolite massifs in central Oman (Fig. 1a). To enable a more-robust comparison between the timing of sole metamorphism and ridge magmatism in northern Oman and the UAE, we dated five gabbroic rocks attributed to the main phase (V1) of ridge magmatism in these areas (13215M07, 13215M09, 131213M02, 131212M01, 131217M03; Fig. 1a, Table 1); samples were collected based on published geologic maps from the Oman and UAE (Goodenough et al., 2010; Styles et al., 2006) governments, and detailed mapping and geochemical studies of the Wadi Rajmi (Usui and Yamazaki, 2010) and Wadi Fizh (Adachi and Miyashita, 2003) areas. We further report new data from a tonalite related to the V1 magmatic event from the Wadi Tayin massif in the southern part of the ophiolite. Single-grain ^{206}Pb/^{238}U dates range from 96.46 ± 0.18 to 95.535 ± 0.063 Ma (Fig. 2, Supplementary Fig. S1, Supplementary Table S1). There are resolvable intra-sample variations in ^{206}Pb/^{238}U dates in some samples, and we interpret the youngest cluster of dates in each sample as the best estimate of the final crystallization age; the weighted mean ^{206}Pb/^{238}U dates for the younger clusters range from 96.039 ± 0.039 to 95.568 ± 0.043 Ma (Supplementary Text). The new dates from the northern part of the ophiolite are coeval with our previous analyses of gabbroic rocks from the southern ophiolite massifs (Rioux et al., 2012, 2013) (weighted mean ^{206}Pb/^{238}U dates of 96.121 ± 0.051 to 95.504 ± 0.031 Ma; Fig. 3), suggesting synchronous spreading and crustal growth along the entire length of the ophiolite. This finding conflicts with data in Styles et al. (2006), which suggest that the late (V2) magmatic series in the UAE was as old as 96.4 Ma, requiring that the V1 magmatism in the UAE occurred prior to 96.4 Ma and pre-dated V1 magmatism in Oman. The single tonalite body we dated in this study from the southern Wadi Tayin massif (1923M12) was previously dated by Tilton et al. (1981), and yielded one of the oldest date in that study (96.9 ± 0.4 Ma); we found a younger date of 96.039 ± 0.039 Ma, which is consistent with the timing of V1 magmatism based on other samples (Fig. 3). The youngest date from our new analyses comes from a gabbroic exposure in the UAE adjacent to a younger magmatic unit, and this sample may be related to secondary V2 magmatism.

To establish the timing of metamorphism within the sole of the ophiolite, we dated samples from the Sumeini and Wadi Tayin metamorphic sole localities (Fig. 1, Table 1, Supplementary Fig. S1, Supplementary Table S1). At the Sumeini locality, two small (~15 cm) diorite pods (13213M05, 13213M06) yielded the most-precise results. Textural evidence and mineralogy—discussed in section 5.2—suggest that these pods crystallized from partial melts formed during metamorphism of the surrounding amphibolite, in agreement with previous work (Cowan et al., 2014; Searle and Malpas, 1980). The two samples yielded tight clusters

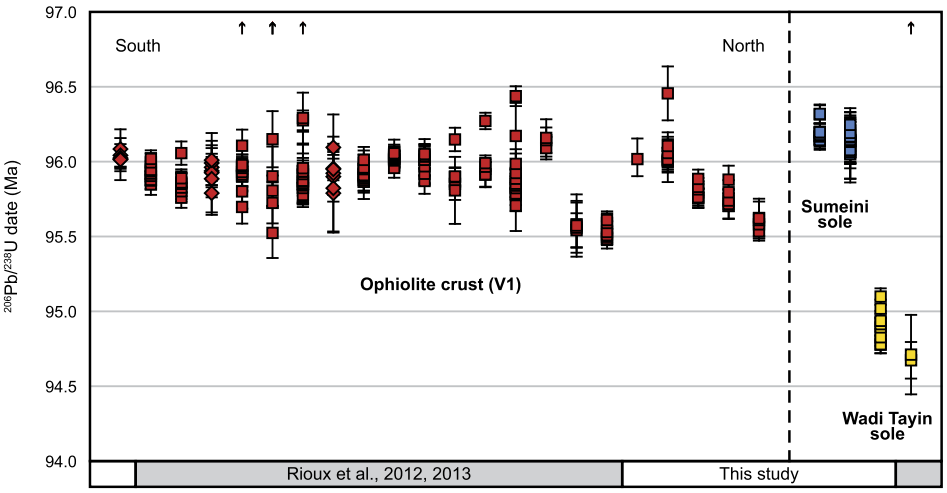

Fig. 3. Summary of Th-corrected zircon $^{206}Pb/^{238}U$ dates from the V1 plutonic crust and metamorphic sole (this study; Rioux et al., 2012, 2013). Each datum and error bar ($\pm 2\sigma$) correspond to a single zircon analysis and clusters of data are analyses from a single sample. Arrows denote samples with inherited older zircons that plot off scale. For the V1 plutonic dates, oxide gabbro samples are plotted as squares and tonalite–trondhjemite samples as diamonds. Dates are in millions of years ago (Ma). Dates from the ophiolite crust are arranged from south to north. Imprecise single zircon dates from this study (Supplementary Text) and our previous research ($2\sigma \geq \pm 0.3$ Ma) were excluded for clarity. Gray and white bars at the bottom of the figure indicate whether the data are from this study (white) or Rioux et al. (2012, 2013) (gray). (A color version of this figure is available with the web version of the article.)

of single zircon dates; 13213M06 yielded a cluster of fifteen analyses with a weighted mean $^{206}Pb/^{238}U$ date of 96.146 ± 0.035 Ma (mean square of the weighted deviates, MSWD = 0.98), and 13213M05 yielded a cluster of seven analyses with a weighted mean $^{206}Pb/^{238}U$ date of 96.169 ± 0.022 Ma (MSWD = 0.66), and two slightly older analyses with $^{206}Pb/^{238}U$ dates of ~96.3 Ma (Fig. 2). The two older dates from 13213M05 likely reflect the presence of older zircon cores, which may have been inherited from the surrounding amphibolite. Four of the zircons within the younger cluster of dates from this sample were imaged by CL prior to the U–Pb analyses (Fig. 4). The CL images do not show any evidence for inherited cores in these grains, supporting the interpretation that the younger cluster of dates records the timing of zircon crystallization from the magma; the two older grains from this sample were not imaged prior to dating. The weighted mean dates from the two dated diorite pods overlap within uncertainty, and suggest that metamorphism at the Sumeini locality occurred at ~96.16 Ma. A texturally late diorite dike that cross cuts the amphibolite foliation at Sumeini (13213M02; Supplementary Fig. S2) yielded a range of lower precision single zircon $^{206}Pb/^{238}U$ dates from 96.41 ± 0.32 to 95.02 ± 0.50 Ma (Fig. 2), suggesting a maximum crystallization age of ~95.0 Ma. The younger date is consistent with the cross-cutting field relations; the date does not constrain the timing of sole metamorphism but places a minimum age on the formation of the amphibolite foliation.

At the Wadi Tayin sole locality, a single diorite pod (~10 cm; 13222M02; Supplementary Fig. S2), attributed to partial melting of the surrounding amphibolite, yielded $^{206}Pb/^{238}U$ dates from 95.099 ± 0.055 to 94.777 ± 0.058 Ma (Fig. 2). The range of dates again suggests that some of the zircons in this sample contain inherited older cores. Four zircons that do not show evidence for inherited older cores in CL define the young end of the age spectrum, with a weighted mean $^{206}Pb/^{238}U$ date of 94.815 ± 0.030 Ma (MSWD = 2.9); other imaged, but undated, grains from this sam-

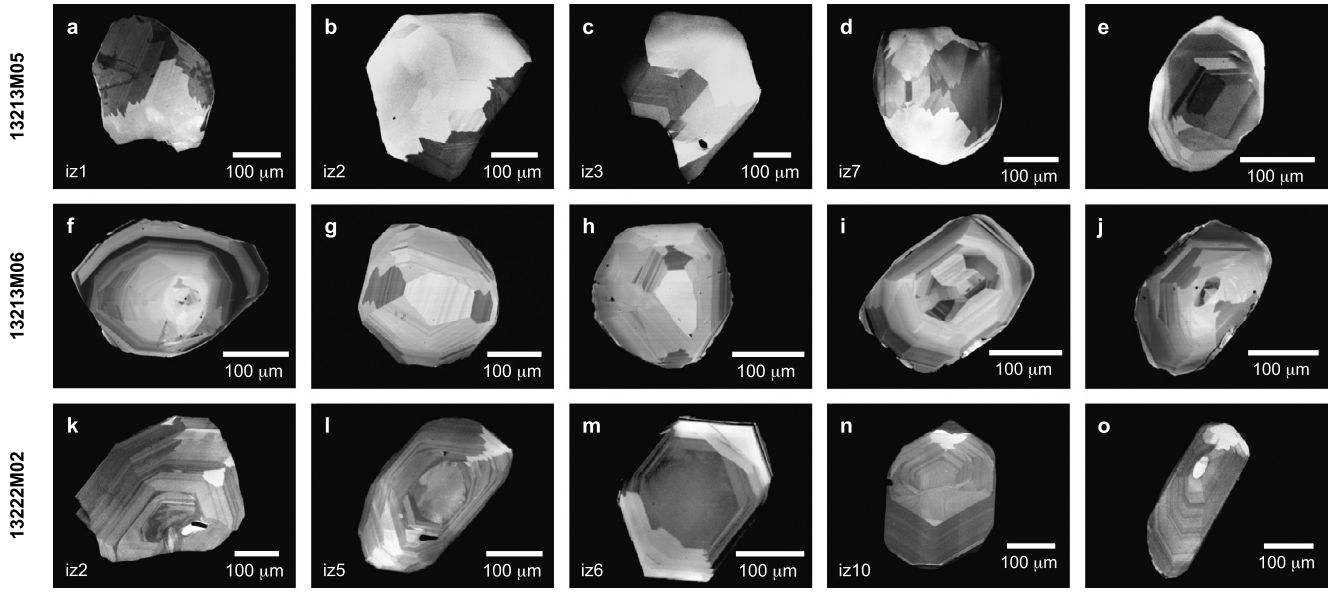

Fig. 4. Representative cathodoluminescence (CL) images of zircons. Imaged grains are from samples 13213M05, 13213M06 and 13222M02. Zircons identified with "iz" were plucked from the mounts and subsequently dated (Supplementary Table 1).

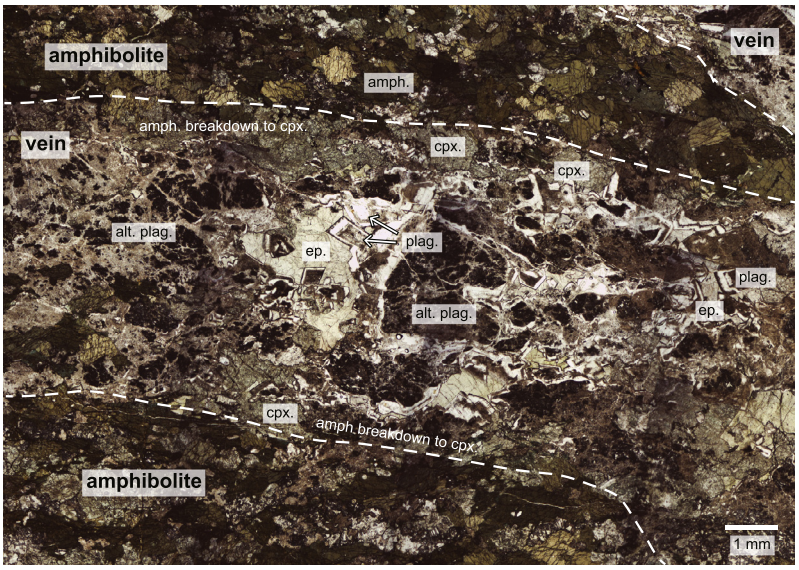

Fig. 5. Plane-polarized light photomicrograph of amphibolite and igneous veins in sample 13213M05. Amphibole breakdown reactions can be seen along the margins of the veins and within the amphibolite. amph., amphibole; cpx., clinopyroxene; ep., epidote; plag., plagioclase; alt. plag., altered plagioclase. (A color version of this figure is available with the web version of the article.)

ple show textures in CL that could record the presence of older cores (Fig. 4o). The new date overlaps with our previous analyses from a trondhjemite pod from Wadi Tayin, which yielded a weighted mean $^{206}Pb/^{238}U$ date of 94.69 ± 0.11 Ma (Fig. 3) (Rioux et al., 2013). The more precise data from this study suggest that peak metamorphism at the Wadi Tayin locality occurred at ~94.82 Ma. Zircons from a garnet amphibolite at Wadi Tayin (13222M08) yielded more-complex results: single zircon $^{206}Pb/^{238}U$ dates range from 96.067 ± 0.068 to 95.085 ± 0.063 Ma (Fig. 2). The large range of dates likely reflect either 1) mixing between new zircon grown during metamorphism and older zircon cores, 2) inheritance of whole grains from the protolith to the amphibolite, or 3) earlier, prograde-to-peak zircons that grew prior to melting of the amphibolite. The data suggest that peak metamorphism occurred after 95.085 ± 0.063 Ma, consistent with the more-precise age constraint from the diorite pod from this locality (13222M02; 94.815 ± 0.030 Ma).

5.2. Textural context of the dated zircons

To understand the implications of our new U–Pb dates, it is necessary to understand the petrogenetic history of the dated rocks. At the Sumeini and Wadi Tayin sole localities, sampled diorite pods contained abundant large zircons and provided the most-precise dates. Here we discuss the origin of the pods, and the distribution of zircons within the dated samples. We focus on observations from the two dated pods that are concordant to the foliation from the Sumeini sole locality (13213M05, 13213M06), which we studied in the most detail.

In the field, the diorite pods are ~15 cm × 5 cm with irregular boundaries. Small stringers (<1 cm) from the pods project into the surrounding amphibolite, and the pods contain numerous cm-scale pieces of the amphibolite (Supplementary Fig. S2). The host amphibolite is composed of foliated amphibole + plagioclase ± clinopyroxene, whereas the pods contain plagioclase (An_{5-15}) + epidote + clinopyroxene (Fig. 5). The plagioclase crystals in the pods are euhedral and have oscillatory zoning with an increasing albite component from core to rim. Epidote crystallized after plagioclase and is interstitial and/or encompasses plagioclase grains. Some epidotes have oscillatory zoning with an increasing clinozoisite component from core to rim. Textural observations suggest that clinopyroxene along the margins of the diorite pods formed as a result of amphibole breakdown (Fig. 5), reflecting either a melting reaction (e.g., Hacker, 1990) or reaction between an intruding melt and the surrounding amphibolite. The presence of euhedral minerals, oscillatory zoning in the plagioclase and epidote, and the absence of foliation in the diorite pods are consistent with crystallization from a magma, in agreement with previous work (Cowan et al., 2014; Searle and Cox, 1999; Searle and Malpas, 1980, 1982); magmatic epidote would have been stable at the inferred peak metamorphic pressures of 11–13 kbar for granulite minerals within the amphibolites (Schmidt and Poli, 2004). The absence of deformation within the pods suggests that either the pods formed near the end of deformation or that the locus of deformation shifted after crystallization. The pods do not contain quartz and have a lower SiO_2 content than expected for low-percentage partial melts of amphibolite, suggesting that they represent cumulates separated from a more Si-rich melt; other crystallized igneous pods from the Sumeini and Wadi Tayin localities contain quartz (Cowan et al., 2014; Searle and Cox, 1999; Searle and Malpas, 1980, 1982).

To determine the petrogenetic setting of the dated zircons from the diorite pods, we used backscattered electron (BSE) imaging of polished slabs (Fig. 6). The fine-scale intermingling of the amphibolite and melt-related pods and veins prohibited complete separation of pods and veins from the amphibolites during mineral separation. However, BSE imaging and energy dispersive spectrometry (EDS) of serial sections of the dated samples from the Sumeini locality reveal that large (>150 μm) zircons, similar to the grains dated in this study, primarily—and perhaps exclusively—occur within the igneous veins. In twelve polished slabs (20 mm × 30–50 mm) of intermingled amphibolite and igneous veins, we identified seven zircons with a maximum dimension >150 μm, seven zircons with a maximum dimension between 75–150 μm and 39 zircons with a maximum dimension <75 μm (Fig. 6). All of the largest zircons (>150 μm), and all but one of the intermediate zircons (75–150 μm) are within veins; the petrographic relationship of the final intermediate zircon is ambiguous. The smaller zircons occur in both the amphibolite and veins. Taken together, the data outlined above suggest that the diorite pods and veins formed by partial melting during metamorphism, and that the dated zircons crystallized from the partial melts, and therefore record the age of peak or post-peak metamorphism.

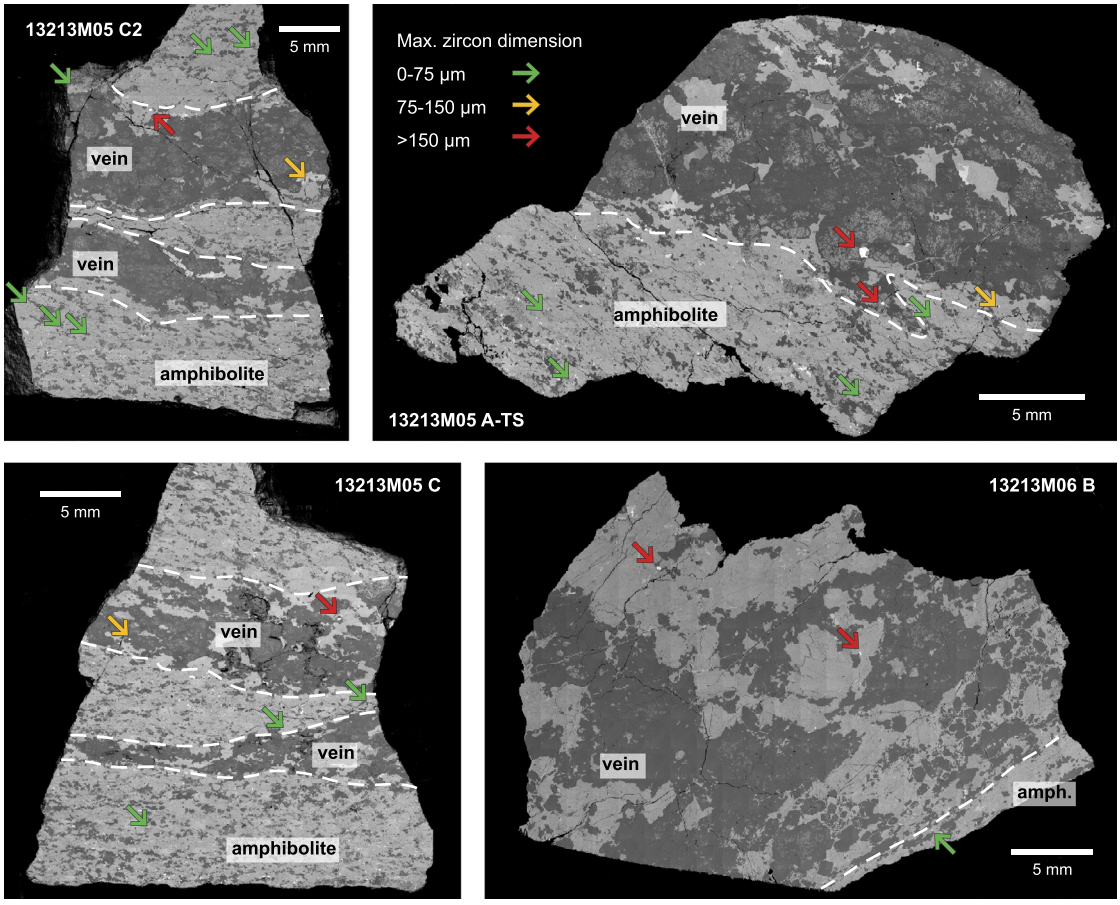

Fig. 6. Backscattered electron (BSE) images showing the distribution of zircons in the dated samples. Images are from polished sections of amphibolite containing igneous veins from samples 13213M05 and 13213M06. Zircons are bright in the BSE images and are marked by colored arrows corresponding to the size of the grains. Large (>150 µm) zircons, similar to the grains dated in this study, primarily—and perhaps exclusively—occur within the veins, suggesting that these zircons crystallized from melt. Zircon identifications were verified using energy dispersive spectrometry (EDS). Unmarked minerals with bright backscatter response are typically Fe oxides. The marked >150 µm zircon in slab 13213M05 C plucked out between imaging sessions, and appears as a hole in the slab. (A color version of this figure is available with the web version of the article.)

5.3. Whole rock Sm–Nd isotopic analyses

Whole rock Sm–Nd isotopic analyses were used to constrain the protolith composition of four samples from the metamorphic sole (Supplementary Table S2). Two garnet amphibolite samples yielded $\varepsilon_{Nd}(96\ Ma)$ of 3.90 ± 0.16 (13213M03) and 7.11 ± 0.16 (13222M08), from Sumeini and Wadi Tayin respectively. A metasedimentary quartz-rich garnet-muscovite schist from within amphibolite at Wadi Tayin yielded $\varepsilon_{Nd}(96\ Ma) = -8.35 \pm 0.05$ (sampled ~25–50 m below the Semail thrust). A texturally late diorite vein from Sumeini (13213M02), which we also dated, yielded $\varepsilon_{Nd}(96\ Ma) = -11.04 \pm 0.49$. In addition, one of the dated V1 gabbros (13215M09) yielded $\varepsilon_{Nd}(96\ Ma) = 7.43 \pm 0.39$; whole rock major and trace element data for this sample are provided in Supplementary Table S3.

6. Discussion

6.1. Interpretation of the whole rock Sm–Nd data

Rocks related to the crust forming V1 magmatic event in the ophiolite have $\varepsilon_{Nd}(96\ Ma)$ of +7 to +9 (Amri et al., 2007; Godard et al., 2006; Rioux et al., 2012, 2013), similar to the isotopic composition of modern MORB (e.g., Hofmann, 2007). The Nd isotopic composition of the V1 gabbro 13215M09 [$\varepsilon_{Nd}(96\ Ma) = 7.43$] overlaps the range defined by previous studies.

The four samples analyzed from the Wadi Tayin and Sumeini localities show a large range in Nd isotopic composition, from $\varepsilon_{Nd}(96\ Ma) = -11.04$ to 7.11. The field relationships and U–Pb dates from the analyzed late diorite vein from the Sumeini locality [$\varepsilon_{Nd}(96\ Ma) = -11.04$] indicate that it significantly postdates peak metamorphism; the vein crosscuts the amphibolite foliation and the U–Pb data suggest a maximum crystallization age >1 Ma younger than the timing of peak metamorphism at Sumeini. The origin of this crosscutting vein is not constrained, and it is not clear how the isotopic composition relates to the protolith composition of the metamorphic rocks within the sole.

The three other samples suggest variable protolith compositions for the sole metamorphic rocks. The garnet amphibolite at the Wadi Tayin locality collected directly below the Semail thrust yielded $\varepsilon_{Nd}(96\ Ma) = 7.11$, similar to the isotopic composition of modern MORB and the ophiolite crust. These data are consistent with trace-element data suggesting that the protoliths to the sole amphibolites consisted of basalts generated along a spreading center (Searle and Cox, 1999, 2002; Searle and Malpas, 1982). In contrast, the metasediment from the Wadi Tayin locality has $\varepsilon_{Nd}(96\ Ma) = -8.35$, suggesting that it includes material with time-integrated light rare earth-element enrichment. We consider it likely that the protolith to the metasediments is a biogenic chert with a small percentage of terrigenous sediment, consistent with the conclusion of Ishikawa et al. (2005). Finally, a garnet amphibolite from Sumeini has $\varepsilon_{Nd}(96\ Ma) = 3.90$. Such low ε_{Nd} are extremely rare at mid-ocean ridges (Hofmann, 2007), and may in-

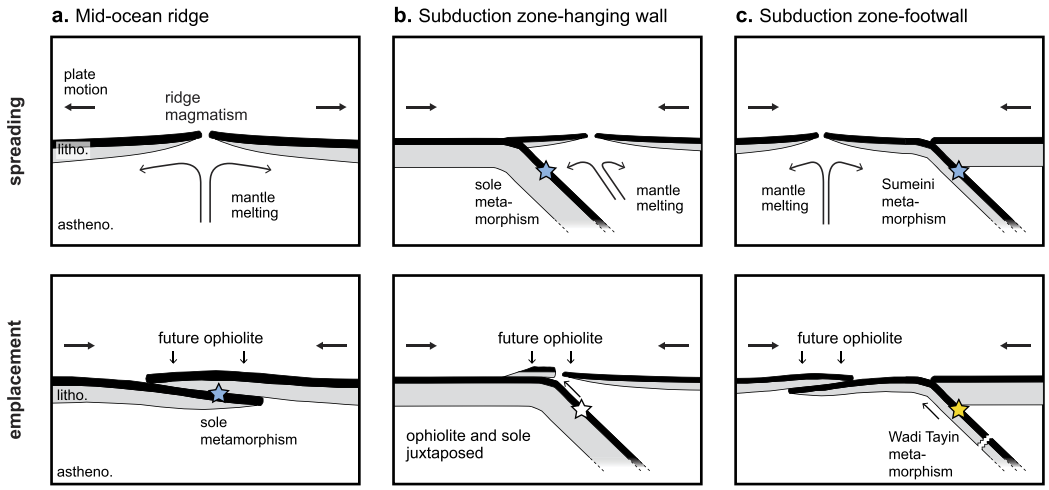

Fig. 7. Models for ophiolite formation. (a) Ophiolites form at mid-ocean ridge spreading centers followed by thrusting at or near the ridge axis (Boudier et al., 1988). (b) Ophiolites form above subduction zones as a result of extension in the over-riding plate (Pearce et al., 1981; Searle and Cox, 2002; Searle and Malpas, 1980, 1982). (c) Ophiolites form in the footwall of subducting plates. Ridge subduction may jam the subduction zone, leading to intra-oceanic thrusting and ophiolite emplacement. Filled stars show the location of active metamorphism of sole rocks; the white star shows the original depth of metamorphism for rocks that were subsequently exhumed. Abbreviations are litho., lithosphere, including the crust (black) and lithospheric mantle (gray); astheno., asthenospheric mantle. (A color version of this figure is available with the web version of the article.)

dicate that the protolith to some of the sole amphibolites are a mix between basaltic and sedimentary components.

6.2. The tectonic setting of ophiolite formation

The tectonic setting during formation of the Semail and other ophiolites has long been contentious. The two most widely cited models for the Semail ophiolite are 1) the ophiolite formed at a normal mid-ocean ridge spreading center and was subsequently thrust over adjacent oceanic crust (Fig. 7a) (Boudier et al., 1988), and 2) the ophiolite formed at a spreading ridge in the hanging wall of a subduction zone (Fig. 7b) (Pearce et al., 1981; Searle and Cox, 2002; Searle and Malpas, 1980, 1982). We further consider a third potential geometry, in which the ophiolite formed on a subducting plate outboard of the subduction trench (Fig. 7c). In the mid-ocean ridge model (Fig. 7a), the calculated pressures in the sole require that the over-thrust slab was $\geq$35 km thick, and was subsequently thinned (Hacker and Gnos, 1997). In the supra-subduction zone model (Fig. 7b), emplacement of the ophiolite is accommodated along the existing subduction zone interface, and the highest-grade sole rocks represent buoyant exhumation of material from deeper in the subduction zone (e.g., Cowan et al., 2014). In the ridge subduction model (Fig. 7c), emplacement of the ophiolite requires development of a new thrust below the future ophiolite that is distinct from the subduction zone interface, potentially as a result of jamming of the subduction zone due to subduction of young buoyant lithosphere as the ridge approaches the trench; the ophiolite could then be thrust either over the hanging wall of the subduction zone or a new thrust could develop in oceanic lithosphere outboard of the ridge axis.

The three tectonic models make testable predictions about the relative timing of formation of the ophiolite crust and development of thrusting or subduction below the ophiolite: in the mid-ocean ridge model, formation of the ophiolite crust predates thrusting below the ophiolite, whereas in the two latter models, subduction—and associated metamorphism—may be synchronous with or predate formation of the ophiolite crust. Our new U–Pb dates indicate that the metamorphic rocks preserved at the Sumeini locality underwent metamorphism and melting at 96.16 Ma, immediately prior to or synchronous with formation of the ophiolite crust at a submarine spreading center between 96.12–95.50 Ma (Fig. 3). These data preclude the traditional mid-ocean ridge model for ophiolite formation (Fig. 7a), and favor the two subduction-related models (Fig. 7b, c).

The geochronologic data alone do not differentiate between a supra-subduction zone and ridge-subduction setting (Fig. 7b, c), and there are viable modern analogues for each model. It has been proposed that ophiolites may form in a range of different supra-subduction zone tectonic settings, including back-arc spreading centers (Pearce et al., 1981), at the intersection of spreading ridges and subduction trenches (Casey and Dewey, 1984), or in the forearc of subduction zones during subduction initiation (e.g., Stern and Bloomer, 1992). For the ridge-subduction model, the southern Chile Ridge, adjacent to the Chile Trench, provides a possible analogue; Klein and Karsten (1995) showed that the geochemical signatures of ridge segments on the southern Chile Ridge near the Chile Trench have been influenced by the adjacent subduction zone. The trace-element patterns from these segments share some similarities with the V1 lavas in Oman (Godard et al., 2006; Karsten et al., 1996; Klein and Karsten, 1995).

We favor a supra-subduction zone model because it more simply explains both the geochemical constraints from the ophiolite and our new U–Pb data. The major element data from the ophiolite in particular strongly favor a supra-subduction zone origin. These data show that the V1 (Geotimes) dikes and lavas in the ophiolite on average have lower TiO_2 at a given MgO, and higher SiO_2 and lower Cr than typical MORB (MacLeod et al., 2013; Pearce et al., 1981). Data from the southern Chile Ridge plot within the MORB field for these elements (Karsten et al., 1996; Sherman et al., 1997), indicating that although near-trench processes can generate mid-ocean ridge segments with trace-element signatures similar to ophiolites, these processes do not reproduce observed major element trends in the Semail ophiolite.

A supra-subduction zone model also provides a simple explanation of the new U–Pb dates from the Wadi Tayin and Sumeini sole localities, and our previous data constraining the age of felsic intrusions within the ophiolite mantle. In Oman and the UAE, a series of granite, granodiorite, tonalite, and trondhjemite sills and dikes intrude mantle harzburgite below the crust–mantle transition (Amri et al., 2007; Rollinson, 2009, 2015). These intrusions have ε_{Nd}(96 Ma) and ε_{Hf}(96 Ma) that are lower than expected for a mid-ocean ridge setting, and are best explained by thrusting or subduction, and partial melting, of terrigenous or pelagic sediments below the ophiolite (Haase et al., 2015; Rioux et al., 2013;

Rollinson, 2009, 2015). In our previous work, we dated one of these intrusions from the Haylayn massif [$\varepsilon_{Nd}(96\ Ma) = -7.7$] and found a date of 95.174 ± 0.039 Ma (Rioux et al., 2013), suggesting the establishment of sub-ophiolite thrusting by this time. In supra-subduction zone models, the dates for sole metamorphism that are older and younger than ridge magmatism (96.16 and 94.82 Ma) and the intrusion of the felsic mantle dikes at 95.2 Ma, can be explained by ongoing metamorphism and sediment melting on a single subducted slab (section 6.3). A ridge-subduction model would require a more complex tectonic development to account for the combined U–Pb datasets.

Overall, while there are complications with all models, a supra-subduction zone model (Fig. 7b) most parsimoniously explains i) our new U–Pb dates from the Sumeini and Wadi Tayin sole localities; ii) observed differences between the major and trace element geochemistry of the ophiolite volcanic rocks (V1 and V2) and modern MORB (Alabaster et al., 1982; Ishikawa et al., 2002; MacLeod et al., 2013; Pearce et al., 1981); iii) compositional differences between the ophiolite crust and metamorphic sole (Searle and Cox, 2002; Searle and Malpas, 1982); iv) the inferred pressures of metamorphism within the ophiolite sole (Cowan et al., 2014); and v) the intrusion of felsic magmas with low ε_{Nd} and ε_{Hf} into the mantle section of the ophiolite soon after ridge magmatism (Haase et al., 2015; Rioux et al., 2013; Rollinson, 2009, 2015).

6.3. Origin of high-grade rocks within the metamorphic sole

Models for the formation of the sole have generally assumed that metamorphism of the highest-grade rocks was synchronous along the length of the ophiolite (Searle and Cox, 2002; Searle et al., 2015). This conclusion has been supported by similarities in the structural position, metamorphic architecture and lower-precision radiometric dates of sole localities along strike (Hacker et al., 1996); thermobarometric results suggest that the highest grade rocks at the Wadi Tayin and Sumeini localities reached similar peak conditions of 1.1–1.2 GPa and 800–900 °C (Cowan et al., 2014), and both localities have a similar pseudostratigraphy, with a m-scale layer of garnet amphibolite/granulite directly below the Semail thrust underlain by garnet-free rocks. However, our new dates show that melting and metamorphism in the Sumeini and Wadi Tayin sole localities occurred diachronously at 96.16 and 94.82 Ma, respectively.

We envision two possible models to explain the combined U–Pb zircon dates and calculated metamorphic pressures in a subduction-zone setting (Fig. 8). In the first model, each sole locality formed from slivers of a subducted slab that reached peak pressures 1.3 Ma apart. Following metamorphism, the metamorphic rocks from the Sumeini and Wadi Tayin localities either returned up the subduction channel at different times (Fig. 8b), or were transferred to the hanging wall of the subduction zone after metamorphism, and later exhumed in a coherent slab of mixed hydrated mantle and metabasalt. Alternately, the diachronous metamorphism may reflect variable subduction rates along the length of the ophiolite—perhaps as a result of jamming of the subduction zone to the north (modern coordinates), which could have led to rotation of the subducted slab (Fig. 8c). In this case, although the metamorphic rocks from the Sumeini locality reached peak pressures at 96.16 Ma, they may have remained at near-constant depth, while the southern portion of the slab continued to subduct. The metamorphic rocks from the Wadi Tayin locality then reached peak pressures at 94.82 Ma, and the rocks from both localities were exhumed in a single coherent piece of the subducted slab.

A key consideration in either model is whether the sole rocks could have been exhumed by buoyancy. To determine the buoyancy of the sole with respect to the overlying mantle peridotite, we generated *P–T* pseudosections in *Perple_X* using an average

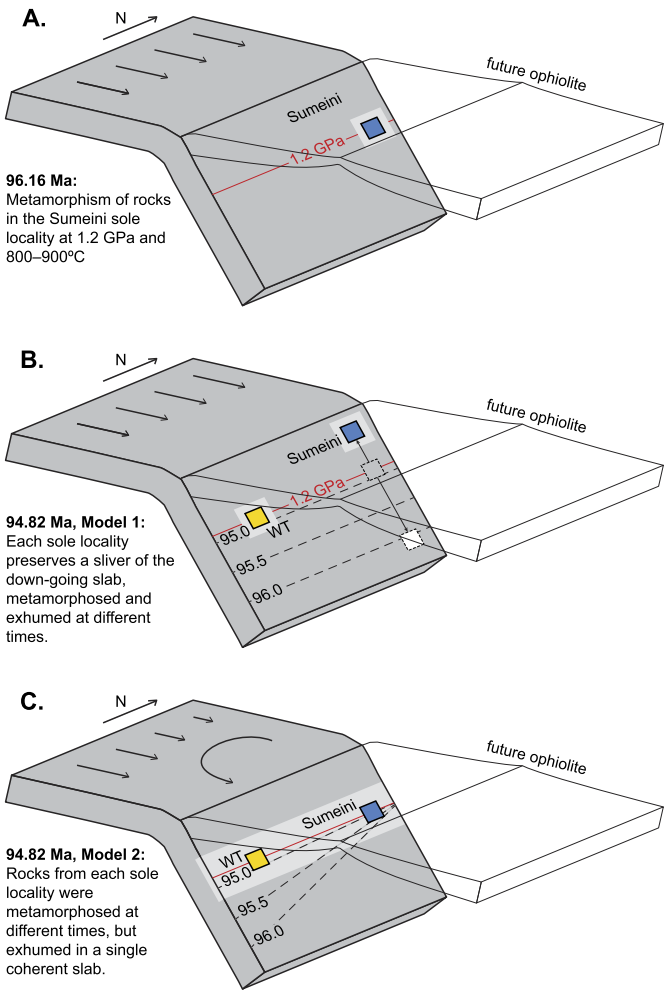

Fig. 8. Models for formation of the metamorphic sole. (a) Formation of the Sumeini amphibolites and granulites at 96.16 Ma and 1.2 GPa. (b) Model 1: If the subduction rate was constant along the length of the ophiolite, each sole locality may preserve a sliver of the subducted plate that underwent metamorphism and returned up the subduction channel at different times. Following metamorphism at 1.2 GPa at 96.16 Ma, the Sumeini metamorphic rocks returned up the subduction channel, prior to metamorphism of rocks from Wadi Tayin at 1.2 GPa at 94.82 Ma. Dashed lines show 1.2 GPa isobars formed at 95.0, 95.5 and 96.0 Ma. (c) Model 2: Subduction is jammed to the north, leading to rotation of the subducting slab and variable subduction rates. In this model, rocks from Sumeini reached 1.2 GPa at 96.16 Ma, but then stalled at that depth. Continued subduction led to metamorphism of the Wadi Tayin rocks at 1.2 GPa at 94.82 Ma. The Sumeini and Wadi Tayin rocks were then exhumed in a coherent slab (light gray). (A color version of this figure is available with the web version of the article.)

bulk composition of sole amphibolite from the Wadi Tayin locality and a harzburgite composition based on an average of whole rock harzburgite analyses from the Wadi Tayin massif (Supplementary Table S4; Supplementary Text). The calculated mineral assemblages are consistent with the observed mineralogy of amphibolite- to granulite-facies rocks from the sole. Calculated densities show that even at the peak granulite-facies conditions reached by the sole rocks (1.2 GPa and 800–900 °C), the garnet granulites were at least 50–75 kg/m^3 less dense than the overlying, hydrated mantle wedge (Fig. 9). Further, the density difference would have increased as the metamorphic rocks rose to lower pressures and underwent retrograde reactions at amphibolite-facies conditions.

The *Perple_X* results indicate that if the granulite- to amphibolite-facies metabasalts in the Sumeini and Wadi Tayin sole localities became detached from the downgoing slab, buoyancy could have driven them to return up the subduction channel. We have

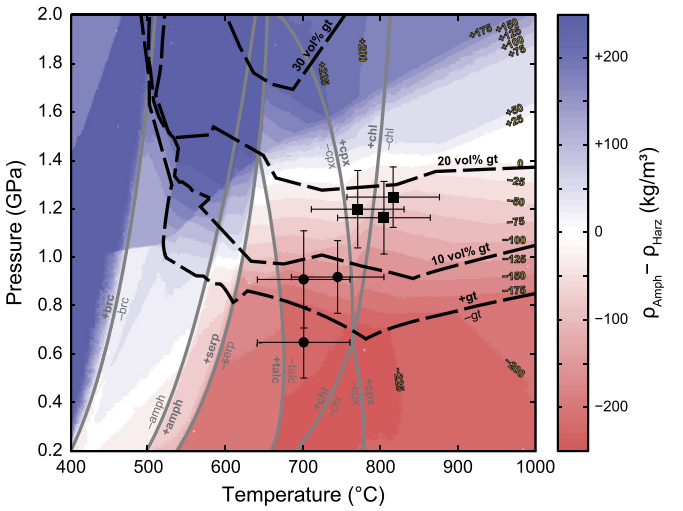

Fig. 9. Density differences between amphibolite- to granulite-facies metabasalt and harzburgite calculated with *Perple_X* (the contour interval is 25 kg/m^3). Blue indicates amphibolite denser than co-existing harzburgite at the equivalent P–T conditions; red the opposite. At low T, the difference is defined by the stability fields of hydrous minerals in the harzburgite (gray solid lines), whereas at higher-T the difference is dominated by the modal abundance of garnet in the amphibolite (black dashed lines). P–T conditions calculated for granulite-facies (boxes) and amphibolite-facies (circles) assemblages in the Wadi Tayin and Sumeini exposures of the metamorphic sole are shown for reference (Cowan et al., 2014); all P–T data plot below the line of equal density, indicating that the amphibolite is positively buoyant with respect to harzburgite. Details of the calculations are provided in the Supplementary Text. (A color version of this figure is available with the web version of the article.)

previously hypothesized that slab breakoff at greater depths could also have resulted in buoyancy driven exhumation of the sole rocks (Searle et al., 2015). We prefer the former non-slab break off model, because high pressure rocks exposed at As Sifah, on the east coast of Oman, provide evidence for continued subduction after exhumation of the sole granulites and amphibolites—eclogites from As Sifah are interpreted to represent continental material subducted to pressures up to 2.5 GPa (e.g., Searle et al., 1994) at ~79 Ma (Warren et al., 2005). A simple explanation for the formation of both the metamorphic sole and the HP rocks is that they formed in a single east dipping (present coordinates) subduction zone (e.g., Searle et al., 1994). The similar ^{40}Ar/^{39}Ar cooling dates from the ophiolite crust and metamorphic sole (Hacker et al., 1996) suggest that the sole rocks returned up the subduction channel, cooled, and were juxtaposed with the base of the ophiolite soon after peak metamorphism. Continued subduction and slab pull may then have led to subduction of the continental margin and final obduction of the ophiolite by ~79 Ma (Warren et al., 2005).

The two models we present for the formation of the Sumeini and Wadi Tayin metamorphic rocks (return of slivers of subducted slab versus slab rotation; Fig. 8) could be tested by additional high-precision dating of other sole localities: the first model predicts a random variation of dates at different sole localities, whereas the second model predicts a smooth spatial progression of ages from north to south. In the latter model, jamming of the subduction zone in the northern part of the ophiolite may help to explain along-strike differences between exposures in Oman and the UAE: as noted above, the proportion of late (V2) igneous rocks increases northward in the ophiolite, perhaps reflecting heating and dehydration of a stalled slab to the north.

In the preceding discussion, we treated the ophiolite as a relatively coherent block formed along a roughly northwest–southeast (current coordinates) striking ridge. Paleomagnetic studies of dikes, lavas, overlying sediments, layered gabbros and peridotites have documented different orientations between the northern and southern massifs, and even within the northern massifs, during the V1 and V2 magmatic events (Perrin et al., 2000; Weiler, 2000). Based on these data it has been proposed that there has been 90–120° of rotation between the northern and southern massifs since formation of the ophiolite. We consider it unlikely that such rotations occurred. Sheeted-dike orientations along the length of the ophiolite are consistently oriented northwest–southeast (Nicolas et al., 2000). Our cumulative U–Pb dataset also shows that both the V1 (96.12–95.50 Ma) and V2 (95.5–95.0 Ma) magmatic series formed synchronously in the southern and northern massifs. It would be fortuitous if the northern and southern massifs formed and were subsequently intruded by later magmatic series over the same short time intervals at separate ridges oriented at >90° to each other, prior to tectonic rotations leading to the current alignment of the ophiolite massifs and sheeted dikes. A simpler explanation is that the ophiolite formed along a single ridge system with limited rotations among the different massifs, and that some or all of the paleomagnetic signal was reset by later magmatic, hydrothermal and/or tectonic events (e.g., Feinberg et al., 1999).

7. Conclusions

New high-precision U–Pb dates provide insight into the origin of the metamorphic sole of the Semail ophiolite, and the tectonic evolution during ophiolite formation and emplacement. Our previous research and new results show that the main portion of the ophiolite crust formed by oceanic spreading from 96.12–95.50 Ma. New dates from leucocratic pods suggest that amphibolite to granulite facies metamorphism occurred at 96.169 ± 0.022 to 96.146 ± 0.035 Ma and 94.815 ± 0.030 Ma in the Sumeini and Wadi Tayin sole localities, respectively. The data from the Sumeini sole locality definitively show for the first time that some sole metamorphism occurred immediately before or during formation of the ophiolite crust. The new U–Pb data—coupled with thermobarometry from the metamorphic sole and existing geochemical data—suggest that sole metamorphism occurred in a subducted slab during ophiolite formation in a supra-subduction zone setting. The 1.3 Ma difference between the Wadi Tayin and Sumeini sole localities suggests that either the metamorphic rocks at these localities underwent metamorphism and returned up the subduction channels at different times, or that differential subduction rates along the length of the ophiolite led to diachronous metamorphism in the subducting slab followed by the exhumation of a single coherent block that was then juxtaposed with the base of the ophiolite.

Acknowledgements

This research was supported by United States National Science Foundation grant EAR-1250522 to Matthew Rioux. We thank Gareth Seward for assistance with the SEM and EPMA at UCSB, Nilanjan Chatterjee for assistance with the SEM at MIT, and Adolphe Nicolas and Françoise Boudier for useful discussions of the data. We thank Mohammed Ali and Aisha Al Suwaidi from The Petroleum Institute for logistical support in the United Arab Emirates and the Director General of Minerals, Ministry of Commerce and Industry of the Sultanate of Oman for allowing us to conduct field work in the Sultanate of Oman. The ASTER GDEM is a product of METI and NASA.

Appendix A. Supplementary material

Supplementary material related to this article can be found online at http://dx.doi.org/10.1016/j.epsl.2016.06.051. These data include a Google map of the sample locations for this study.

References

Adachi, Y., Miyashita, S., 2003. Geology and petrology of the plutonic complexes in the Wadi Fizh area: multiple magmatic events and segment structure in the northern Oman ophiolite. Geochem. Geophys. Geosyst. 4, 8619.

Alabaster, T., Pearce, J.A., Malpas, J., 1982. The volcanic stratigraphy and petrogenesis of the Oman ophiolite complex. Contrib. Mineral. Petrol. 81, 168–183.

Amri, I., Ceuleneer, G., Benoit, M., Python, M., Puga, E., Targuisti, K., 2007. Genesis of granitoids by interaction between mantle peridotites and hydrothermal fluids in oceanic spreading setting in the Oman ophiolite. Geogaceta 42, 23–26.

Boudier, F., Ceuleneer, G., Nicolas, A., 1988. Shear zones, thrusts and related magmatism in the Oman ophiolite: initiation of thrusting on an oceanic ridge. Tectonophysics 151, 275–296.

Boudier, F., Nicolas, A., Ildefonse, B., 1996. Magma chambers in the Oman ophiolite: fed from the top and the bottom. Earth Planet. Sci. Lett. 144, 239–250.

Casey, J.F., Dewey, j.f., 1984. Initiation of subduction zones along transform and accreting plate boundaries, triple-junction evolution, and forearc spreading centres—implications for ophiolitic geology and obduction. GSL Spec. Publ. 13, 269–290.

Cowan, R.J., Searle, M.P., Waters, D.J., 2014. Structure of the metamorphic sole to the Oman ophiolite, Sumeini Window and Wadi Tayyin: implications for ophiolite obduction processes. GSL Spec. Publ. 392, 155–175.

Ernewein, M., Pflumio, C., Whitechurch, H., 1988. The death of an accretion zone as evidenced by the magmatic history of the Sumail ophiolite (Oman). Tectonophysics 151, 247–274.

Feinberg, H., Horen, H., Michard, A., Saddiqi, O., 1999. Obduction-related remagnetization at the base of an ophiolite: paleomagnetism of the Samail nappe lower sequence and of its continental substratum, southeast Oman Mountains. J. Geophys. Res. 104, 17703–17714.

Gnos, E., 1998. Peak metamorphic conditions of Garnet amphibolites beneath the Semail ophiolite: implications for an inverted pressure gradient. Int. Geol. Rev. 40, 281–304.

Godard, M., Bosch, D., Einaudi, F., 2006. A MORB source for low-Ti magmatism in the Semail ophiolite. Chem. Geol. 234, 58–78.

Goodenough, K., Styles, M., Schofield, D., Thomas, R., Crowley, Q., Lilly, R., McKervey, J., Stephenson, D., Carney, J., 2010. Architecture of the Oman–UAE ophiolite: evidence for a multi-phase magmatic history. Arab. J. Geosci. 3, 439–458.

Haase, K.M., Freund, S., Beier, C., Koepke, J., Erdmann, M., Hauff, F., 2016. Constraints on the magmatic evolution of the oceanic crust from plagiogranite intrusions in the Oman ophiolite. Contrib. Mineral. Petrol. 171, 1–16.

Haase, K.M., Freund, S., Koepke, J., Hauff, F., Erdmann, M., 2015. Melts of sediments in the mantle wedge of the Oman ophiolite. Geology 43 (4), 275–278.

Hacker, B.R., 1990. Amphibolite-facies-to-granulite-facies reactions in experimentally deformed, unpowdered amphibolite. Am. Mineral. 75, 1349–1361.

Hacker, B.R., Gnos, E., 1997. The conundrum of samail: explaining the metamorphic history. Tectonophysics 279, 215–226.

Hacker, B.R., Mosenfelder, J.L., 1996. Metamorphism and deformation along the emplacement thrust of the Samail ophiolite, Oman. Earth Planet. Sci. Lett. 144, 435–451.

Hacker, B.R., Mosenfelder, J.L., Gnos, E., 1996. Rapid emplacement of the Oman ophiolite: thermal and geochronologic constraints. Tectonics 15, 1230–1247.

Hofmann, A.W., 2007. Sampling mantle heterogeneity through oceanic basalts: isotopes and trace elements. In: Heinrich, D.H., Karl, K.T. (Eds.), Treatise on Geochemistry. Pergamon, Oxford, pp. 1–44.

Ishikawa, T., Fujisawa, S., Nagaishi, K., Masuda, T., 2005. Trace element characteristics of the fluid liberated from amphibolite-facies slab: inference from the metamorphic sole beneath the Oman ophiolite and implication for boninite genesis. Earth Planet. Sci. Lett. 240, 355–377.

Ishikawa, T., Nagaishi, K., Umino, S., 2002. Boninitic volcanism in the Oman ophiolite: implications for thermal condition during transition from spreading ridge to arc. Geology 30, 899–902.

Karsten, J.L., Klein, E.M., Sherman, S.B., 1996. Subduction zone geochemical characteristics in ocean ridge basalts from the southern Chile Ridge: implications of modern ridge subduction systems for the Archean. Lithos 37, 143–161.

Kelemen, P.B., Koga, K., Shimizu, N., 1997. Geochemistry of gabbro sills in the crust–mantle transition zone of the Oman ophiolite: implications for the origin of the oceanic lower crust. Earth Planet. Sci. Lett. 146, 475–488.

Klein, E.M., Karsten, J.L., 1995. Ocean-ridge basalts with convergent-margin geochemical affinities from the Chile Ridge. Nature 374, 52–57.

MacLeod, C.J., Lissenberg, C.J., Bibby, L.E., 2013. "Moist MORB" axial magmatism in the Oman ophiolite: the evidence against a mid-ocean ridge origin. Geology 41 (4), 459–462.

Mattinson, J.M., 2005. Zircon U/Pb chemical abrasion (CA-TIMS) method: combined annealing and multi-step partial dissolution analysis for improved precision and accuracy of zircon ages. Chem. Geol. 220, 47–66.

Nicolas, A., Boudier, F., Ildefonse, B., Ball, E., 2000. Accretion of Oman and United Arab Emirates ophiolite – discussion of a new structural map. Mar. Geophys. Res. 21, 147–180.

Nicolas, A., Reuber, I., Benn, K., 1988. A new magma chamber model based on structural studies in the Oman ophiolite. Tectonophysics 151, 87–105.

Pallister, J.S., Hopson, C.A., 1981. Samail ophiolite plutonic suite: field relations, phase variation, cryptic variation and layering, and a model of a spreading ridge magma chamber. J. Geophys. Res. 86, 2593–2644.

Pearce, J.A., Alabaster, T., Shelton, A.W., Searle, M.P., 1981. The Oman ophiolite as a Cretaceous arc–basin complex: evidence and implications. Philos. Trans. R. Soc. Lond. Ser. A, Math. Phys. Sci. 300, 299–317.

Perrin, M., Plenier, G., Dautria, J.M., Cocuaud, E., Prévot, M., 2000. Rotation of the Semail ophiolite (Oman): additional paleomagnetic data from the volcanic sequence. Mar. Geophys. Res. 21, 181–194.

Quick, J.E., Denlinger, R.P., 1993. Ductile deformation and the origin of layered gabbro in ophiolites. J. Geophys. Res. 98, 14015–14027.

Rioux, M., Bowring, S.A., Kelemen, P.B., Gordon, S., Dudás, F., Miller, R., 2012. Rapid crustal accretion and magma assimilation in the Oman-U.A.E. ophiolite: high precision U–Pb zircon geochronology of the gabbroic crust. J. Geophys. Res. 117.

Rioux, M., Bowring, S., Kelemen, P., Gordon, S., Miller, R., Dudás, F., 2013. Tectonic development of the Samail ophiolite: high-precision U–Pb zircon geochronology and Sm–Nd isotopic constraints on crustal growth and emplacement. J. Geophys. Res. 118, 2085–2101.

Rollinson, H., 2009. New models for the genesis of plagiogranites in the Oman ophiolite. Lithos 112, 603–614.

Rollinson, H., 2015. Slab and sediment melting during subduction initiation: granitoid dykes from the mantle section of the Oman ophiolite. Contrib. Mineral. Petrol. 170, 1–20.

Schmidt, M.W., Poli, S., 2004. Magmatic epidote. Rev. Mineral. Geochem. 56, 399–430.

Searle, M., Cox, J., 1999. Tectonic setting, origin, and obduction of the Oman ophiolite. Geol. Soc. Am. Bull. 111, 104–122.

Searle, M., Cox, J., 2002. Subduction zone metamorphism during formation and emplacement of the Semail ophiolite in the Oman Mountains. Geol. Mag. 139, 241–255.

Searle, M.P., Malpas, J., 1980. The structure and metamorphism of rocks beneath the Semail ophiolite of Oman and their significance in ophiolite obduction. Trans. R. Soc. Edinb. Earth Sci. 71, 247–262.

Searle, M.P., Malpas, J., 1982. Petrochemistry and origin of sub-ophiolitic metamorphic and related rocks in the Oman Mountains. J. Geol. Soc. 139, 235–248.

Searle, M.P., Waters, D.J., Garber, J.M., Rioux, M., Cherry, A.G., Ambrose, T.K., 2015. Structure and metamorphism beneath the obducting Oman ophiolite: evidence from the Bani Hamid granulites, northern Oman mountains. Geosphere 11 (6), 1812–1836.

Searle, M.P., Waters, D.J., Martin, H.N., Rex, D.C., 1994. Structure and metamorphism of blueschist–eclogite facies rocks from the northeastern Oman Mountains. J. Geol. Soc. 151, 555–576.

Sherman, S.B., Karsten, J.L., Klein, E.M., 1997. Petrogenesis of axial lavas from the southern Chile Ridge: major element constraints. J. Geophys. Res. 102, 14963–14990.

Stern, R.J., Bloomer, S.H., 1992. Subduction zone infancy: examples from the Eocene Izu–Bonin–Mariana and Jurassic California arcs. Geol. Soc. Am. Bull. 104, 1621–1636.

Styles, M.T., Ellison, R.A., Phillips, E.R., Arkley, S., Schofield, D.I., Thomas, R.J., Goodenough, K.M., Farrant, A.R., McKervey, J.A., Crowley, Q.G., Pharaoh, T.C., 2006. The Geology and Geophysics of the United Arab Emirates, vol. 2. Ministry of Energy, United Arab Emirates, Abu Dhabi.

Tilton, G.R., Hopson, C.A., Wright, J.E., 1981. Uranium-lead isotopic ages of the Samail ophiolite, Oman, with applications to Tethyan ocean ridge tectonics. J. Geophys. Res. 86, 2763–2775.

Usui, Y., Yamazaki, S., 2010. Salvaging primary remanence from hydrothermally altered oceanic gabbros in the Oman ophiolite: a selective destructive demagnetization approach. Phys. Earth Planet. Inter. 181, 1–11.

Warren, C., Parrish, R., Waters, D., Searle, M., 2005. Dating the geologic history of Oman's Semail ophiolite: insights from U–Pb geochronology. Contrib. Mineral. Petrol. 150, 403–422.

Weiler, P.D., 2000. Differential rotations in the Oman ophiolite: paleomagnetic evidence from the southern massifs. Mar. Geophys. Res. 21, 195–210.